Inorganic Chemistry

pubs.acs.org/IC Article

Pyrrophens: Pyrrole-Based Hexadentate Ligands Tailor-Made for Uranyl (UO_2^{2+}) Coordination and Molecular Recognition

Jacob T. Mayhugh,[‡] Julie E. Niklas,[‡] Madeleine G. Forbes, John D. Gorden, and Anne E. V. Gorden*

Cite This: https://dx.doi.org/10.1021/acs.inorgchem.0c00439 Read Online

ACCESS | Metrics & More | Article Recommendations | Supporting Information

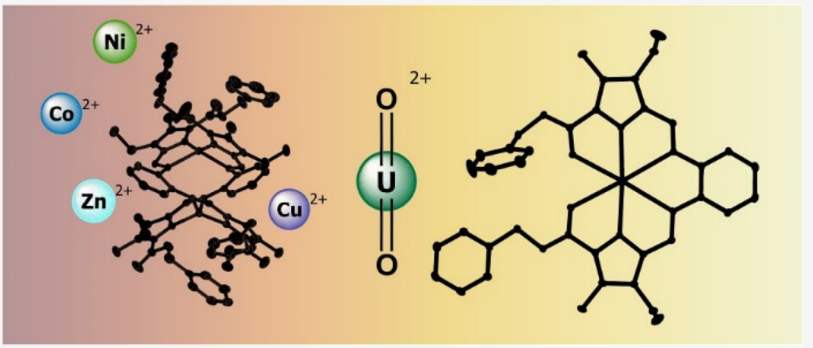

ABSTRACT: Derivatives of a novel pyrrole-containing Schiff base ligand system (called "pyrrophen") are presented which feature substituted phenylene linkers ($R^1 = R^2 = H$ ($\mathbf{H_2L^1}$); $R^1 = R^2 = CH_3$ ($\mathbf{H_2L^2}$)) and a binding pocket modeled after macrocyclic species. These ligands bind neutral CH_3OH in the solid state through pyrrolic hydrogen-bonding. The interaction of the uranyl cation (UO_2^{2+}) and $\mathbf{H_2L^{1-2}}$ yields planar hexagonal bipyramdial uranyl complexes, while the Cu^{2+} and Zn^{2+} complexes were found to self-assemble as dinuclear helicate complexes (M_2L_2) with $\mathbf{H_2L^1}$ under identical conditions. The favorable binding of UO_2^{2+} over Zn^{2+} provides insight into the molecular recognition of uranyl over other metal species. Structural features of these complexes are examined with special attention to features of the UO_2^{2+} coordination environment which distinguish them from other related salophen and porphyrinoid complexes.

INTRODUCTION

In f-element coordination chemistry, the linear uranyl cation (UO_2^{2+}) is generally characterized as a hard acceptor based on Pearson's HSAB (hard−soft acid−base) principle, owing to its highly Lewis acidic and oxophilic nature.[1−3] Current research topics of interest include novel ligands that contain hard donor heteroatoms for sensing or extraction of uranyl (UO_2^{2+}) from aqueous environments; however, many of these systems are indiscriminate toward other cations[4,5] or would not be industrially viable in environmental systems.[6−8] Ligands such as salens, as well as other mixed N/O-donor systems, have been targeted and more extensively studied for their potential to achieve actinide-selective extractions from An^{3+}/Ln^{3+} mixtures,[9] taking advantage of the relative softness and covalency of the trivalent 5f ions.[10] The strategy of employing softer donor ligands for the selective binding, chemosensing, or simply the study of coordination complexes of hexavalent UO_2^{2+}, though, has been largely unexplored. One exception is expanded-porphyrin macrocycles, which have advantageously large molar absorptivities and have been shown to be suitable hosts for uranyl and other actinyl cations, though they suffer from unfavorable kinetics and can be synthetically challenging to prepare.[11−16] Systems with greater flexibility, such as "pacman" Schiff base-expanded polypyrrole macrocycles have been studied as well, as they support unusual oxo-ligand behaviors that are not typically accessible in standard porphyrinoid complexes.[17−19]

The synthetic accessibility and modularity of salen-type Schiff base ligands have made them attractive targets for potential use in separations applications; however, their affinity for a panoply of cations often precludes them from use when selective coordination is desired.[4,20] Recently, a new class of ligands has been reported which utilizes a similar synthetic methodology but replaces the salicylaldehyde with an ester-substituted pyrrol-2-yl analogue.[21] These species are of interest for understanding self-assembly and molecular recognition.[22−25] Previous reports focus on changes in the system's architecture which result from altering the enediamine spacer unit or the pyrrolic arms. Most notably, these ligands self-

Received: February 12, 2020

https://dx.doi.org/10.1021/acs.inorgchem.0c00439
Inorg. Chem. XXXX, XXX, XXX−XXX

Scheme 1. Coordination Modes of Pyrrophen

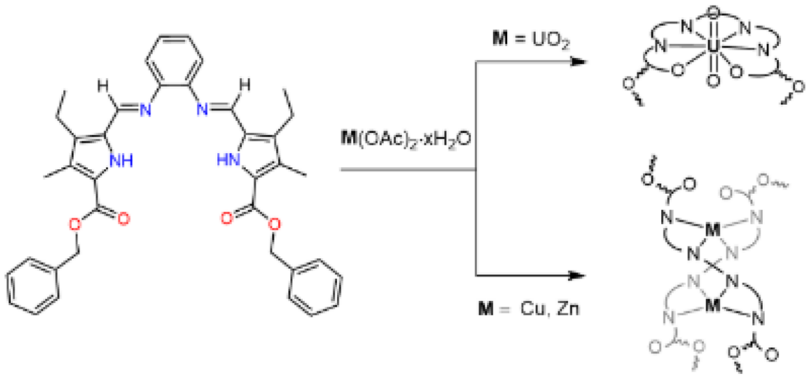

assemble with Cu^{2+} and Zn^{2+} to form M_2L_2 helicate structures through the coordination of the N-donor atoms exclusively.[21,26] Previously, Mn complexes of salen- and salophen-type pyrrolic ligands lacking the bulky ester substituents have been investigated, which adopt a helical architecture with the more flexible ethylenediamine-derived backbone and mononuclear species with the more rigid phenylenediamine backbone.[27] Similar transition metal helicates of dipyrrin-type meso-bridged iminopyrrole ligands have also been observed.[28] Both the Cu^{2+} and Zn^{2+} cations have ionic radii and charge-to-radius ratios similar to that of uranyl (UO_2^{2+}),[29,30] but the affinity of this ligand ($\mathbf{H_2L}$) toward uranyl, to the best of our knowledge, has not been investigated. Given the presence of six suitable donor atoms in this pyrrolic salophen-type system (akin to expanded-porphyrin analogs), its utilization in uranyl coordination was of interest. As this system is macro*a*cyclic, it presents a unique opportunity to explore the bridging of the salen-type and extended porphyrin-type systems to form a new class of ligand that effectively coordinates the uranyl cation while utilizing a softer donor to increase its relative discrimination. The ability to tune the ligand by altering the substitution presents opportunities for improved coordination kinetics over those of macrocyclic species and for improved binding with uranyl versus other metals. Here, we present two bench-stable benzyl ester derivatives of a previously reported ethyl ester bis(pyrrole)phenylenediamine ligand system ($\mathbf{H_2L^1}$ and $\mathbf{H_2L^2}$),[21] which we have nicknamed "pyrrophen," new uranyl and transition metal complexes, and describe the features that make this framework particularly suitable for uranyl coordination (see Scheme 1).

EXPERIMENTAL METHODS

General Considerations. ***Caution!*** *The uranium metal salt—$UO_2(OAc)_2{\cdot}2H_2O$—used in this study contained depleted uranium. Standard precautions for handling radioactive materials or heavy metals such as uranyl nitrate and lead sulfate were followed.*

All ^{1}H NMR spectra were recorded on a Bruker AV 400 MHz or Bruker AV 600 MHz spectrometer, reported in parts per million (δ, ppm) and referenced to residual protio-solvent ($CDCl_3$, δ 7.27, ^{1}H; 77.16, ^{13}C) or tetramethylsilane (TMS, δ 0.00). Deuterated chloroform ($CDCl_3$) was obtained from Cambridge Isotopes Laboratories, Inc., Andover, Massachusetts, and used without further purification. High-resolution mass spectrometry (HRMS) was performed using a quadrupole time-of-flight spectrometer (Q- TOF Premier, Waters) with electrospray ionization (ESI). Elemental analysis (C,H,N) was performed by Atlantic Microlab, Norcross, GA, and was collected in duplicate and reported as an average with the exception of H_2L^2, for which there was not a sufficient sample for duplicate analyses. Samples were dried overnight at 60 °C under a vacuum to remove residual solvent prior to analysis except for H_2L^1 and H_2L^2, which are unstable to heating and have associated solvent, leading to larger errors. Low hydrogen content is observed for duplicate samples of $Cu_2(L^1)_2$—no cause has been identified. Values are inconsistent with the inclusion of residual solvent or associated anions. $UO_2(L^1)$ has lowest errors for a moiety formula including one additional hydrogen atom, though no such proton is observed by any spectroscopic method. All chemicals and solvents were used as received from commercial sources, unless otherwise stated. All solution-phase absorbance spectra were collected from 1000 to 200 nm on a VARIAN Cary 50 WinUV Spectrometer with a xenon lamp using a 1 cm path length quartz cuvette. Titration studies were performed using Teflon capped cuvettes to minimize evaporation of volatile solvent over the course of the experiment. Binding constants were calculated using the program Bindfit from supramolecular.org.[31]

*Benzyl 4-Acetyl-3,5-dimethyl-1H-pyrrole-2-carboxylate (**1**).* Compound **1** was synthesized using modifications of a known procedure.[32] A cold solution of sodium nitrite (8.7 g, 0.13 mol) in water (12 mL) was added dropwise to a stirring solution of benzyl acetoacetate (22.5 mL, 0.13 mol) in acetic acid (28 mL) at 0 °C. Once added, the solution was allowed to warm to room temperature and stirred overnight. Acetylacetone (13.0 mL, 0.13 mol) and additional acetic acid (48 mL) were added to the solution, and the flask was cooled in an ice bath while zinc powder (33 g, 0.50 mol) was added slowly. The reaction flask was then equipped with a condenser and heated to 100 °C for 1 h in an oil bath. The hot solution was poured over ice−water to quench the reaction. The resulting precipitate was collected via vacuum filtration and washed with additional deionized water. The solid was dissolved in hot ethanol, then filtered while hot to remove any remaining zinc. Crystallization from ethanol gave compound **1** as a white solid (25.2 g, 71%). ^{1}H NMR (400 MHz, $CDCl_3$): δ 2.45 (s, 3H), 2.51 (s, 3H), 2.62 (s, 3H), 5.33 (s, 2H), 7.45−7.33 (m, 5H), 9.04 (brs, 1H).

*Benzyl 4-Ethyl-3,5-dimethyl-1H-pyrrole-2-carboxylate (**2**).* Compound **2** was synthesized using modifications of a known procedure.[32] A reaction flask was charged with a magnetic stir bar, **1** (24.4 g, 0.09 mol), sodium borohydride (8.0 g, 0.21 mol), and THF (240 mL) and stirred at room temperature. The flask was then equipped with a dropping funnel containing boron trifluoride diethyl etherate (53 mL, 0.43 mol). The entire system was kept under a constant stream of nitrogen. The $BF_3{\cdot}OEt_2$ was added dropwise over the course of 1 h. After the addition was completed, the mixture was stirred for an additional hour. The reaction was then quenched with the slow addition of 10% HCl in water (until neutral) and extracted three times with chloroform. The organic layers were collected and evaporated to dryness under reduced pressure. The crude solid was then dissolved in 400 mL of 80% ethanol in water and stored in a refrigerator overnight. Compound **2** is collected as a white, needle-like crystalline precipitate from this solution (18.9 g, 82%). ^{1}H NMR (400 MHz, $CDCl_3$): δ 1.05 (t, J = 7.6 Hz, 3H), 2.20 (s, 3H), 2.30 (s, 3H), 2.38 (q, J = 7.5 Hz, 2H), 5.30 (s, 2H), 7.45−7.31 (m, 5H), 8.52 (brs, 1H).

https://dx.doi.org/10.1021/acs.inorgchem.0c00439
Inorg. Chem. XXXX, XXX, XXX−XXX

*Benzyl 4-Ethyl-5-formyl-3-methyl-1H-pyrrole-2-carboxylate (**3**).* Compound **3** was synthesized using modifications of a known procedure.[33] Compound **2** (3.0 g, 12 mmol) was dissolved in a mixture of THF (125 mL), acetic acid (32 mL), and water (32 mL) and vigorously stirred at room temperature. To this mixture, cerium(IV) ammonium nitrate (28.2 g, 51 mmol) was added in a single portion. The reaction allowed to stir for 20 min before being poured into water (250 mL) and extracted three times with chloroform. The organic layers were combined, washed with saturated sodium bicarbonate, and passed through a pad of silica gel. The solution was then concentrated by means of a rotary evaporator and triturated with hexanes to give **3** as an off-white powder which was collected by filtration (2.6 g, 83%). ^{1}H NMR (400 MHz, $CDCl_3$): δ 1.20 (t, J = 7.6 Hz, 3H), 2.31 (s, 3H), 2.75 (q, J = 7.6 Hz, 2H), 5.34 (s, 2H), 7.45−7.35 (m, 5H), 9.44 (brs, 1H), 9.77 (s, 1H).

(Dibenzyl 5,5′-((1E,1′E)-(1,2-Phenylene Bis(azanylylidene))bis-(methanylylidene))bis(4-ethyl-3-methyl-1H-pyrrole-2-carboxylate)) (Pyrrophen, H_2L^1). Pyrrophen was synthesized using a modification from a known procedure.[26] To a solution containing compound **3** (1.1 g, 4.1 mmol) dissolved in a minimum amount of methanol, *o*-phenylenediamine (0.22 g, 2 mmol) was added as a solid. The flask was loosely capped and the mixture stirred at room temperature. After 2 h, the ligand precipitated as a yellow powder; however, the reaction was allowed to stir overnight to go to completion. The product was collected by vacuum filtration (1.00 g, 82%), washed with methanol and ethanol, and used directly for metal complexation without further purification. ^{1}H NMR (400 MHz, $CDCl_3$): δ 1.08 (t, J = 7.5 Hz, 6H), 2.32 (s, 6H), 2.59 (q, J = 7.6 Hz, 4H), 5.31 (s, 4H), 7.12−7.06 (m, 2H), 7.26−7.21 (m, 2H), 7.43−7.28 (m, 10H), 8.30 (s, 2H), 9.71 (brs, 2H). ^{13}C NMR (600 MHz, $CDCl_3$): δ 10.10, 16.44, 17.07, 66.07, 120.26, 122.31, 126.75, 127.05, 128.30, 128.42, 128.67, 129.33, 133.05, 136.30, 145.05, 148.98, 161.05. FT-IR (ATR): 1696 cm^{-1} (s), νC═O; 1610 cm^{-1} (m), νC═N. Anal. calcd for $C_{38}H_{38}N_4O_4\cdot CH_3OH$: C, 72.42; H, 6.52; N, 8.66. Found: C, 72.27; H, 6.48; N, 8.84. λ_{max}: 328 nm (42 800 M^{-1} cm^{-1}). HRMS (ESI) calcd for $C_{38}H_{39}N_4O_4$ ([M + H]$^+$): m/z 615.2971. Found: 615.2977. CCDC 1936495.

Synthesis of Dibenzyl 5,5′-((1E,1′E)-((4,5-Dimethyl-1,2-phenylene)bis(azanylylidene))-bis(methanylylidene))bis(4-ethyl-3-methyl-1H-pyrrole-2-carboxylate) (Me_2Pyrrophen, H_2L^2). Dimethylpyrrophen was synthesized using a modification from a known procedure.[3] To a solution containing compound **3** (0.171 g, 0.63 mmol) dissolved in a minimum amount of methanol, 4,5-dimethyl-*o*-phenylenediamine (0.041 g, 0.3 mmol) was added as a solid, and the mixture was stirred at room temperature. Once completely dissolved, one drop of acetic acid was added and the flask closely capped. The reaction was stirred for an additional 30 min, and the orange solution was then left to sit capped and undisturbed at room temperature for 48 h during which time a large crop of orange-yellow crystals formed and were collected by vacuum filtration using a short-stemmed pipet and washed with methanol. Prior to filtration, a single crystal suitable for X-ray diffraction was isolated from the solution (yield: 0.134 g, 69.4%). ^{1}H NMR (600 MHz, $CDCl_3$): δ 1.09 (t, J = 7.45 Hz, 6H), 2.30 (d, J = 1.72 Hz, 12H), 2.59 (q, J = 7.51 Hz), 3.46 (s, 2H), 5.28 (s, 4H), 6.90 (s, 2H), 7.26−7.41 (m, 10H), 8.31 (s, 2H), 10.25 (bs, 2H). ^{13}C NMR (600 MHz, $CDCl_3$): δ 10.12, 16.43, 17.06, 19.58, 66.03, 121.53, 122.00, 127.12, 128.30, 128.43, 128.68, 129.51, 132.62, 135.25, 136.34, 142.59, 148.36, 161.01. FT-IR (ATR): 1690 cm^{-1} (s), νC═O; 1607 cm^{-1} (m), νC═N. Anal. calcd for $C_{40}H_{42}N_4O_4\cdot CH_3OH$: C, 72.97; H, 6.87; N, 8.30. Found: C, 73.03; H, 6.95; N, 8.45. λ_{max}: 319 nm (49 000 M^{-1} cm^{-1}). HRMS (ESI+) calculated for $C_{40}H_{43}N_4O_4$ ([M + H]$^+$): m/z 643.3284. Found: 643.3288. CCDC 1971893.

Synthesis of Metal Complexes. *Synthesis of $Zn_2(L^1)_2$.* H_2L^1 (0.100 g, 0.164 mmol) was dissolved in 21 mL of a 20:1 THF/MeOH (v/v) solution in a 50 mL round-bottom flask at room temperature and stirred. $Zn(OAc)_2\cdot 2H_2O$ (0.043 g, 0.197 mmol, 1.2 equiv) was added as a solid, causing a color change from bright yellow to intense orange. The flask was loosely capped and stirred at room temperature for 2 h before being reduced to a concentrate using a rotary evaporator, then stored at 0 °C overnight. The complex was collected as a bright orange crystalline powder by vacuum filtration (yield: 0.070 g, 63%). ^{1}H NMR (400 MHz, $CDCl_3$): δ 1.09 (t, 6H), 2.16 (s, 6H), 2.48 (m, 4H), 4.27 (m, 2H), 5.21 (m, 2H), 6.42 (m, 2H), 6.77 (m, 4H), 6.88 (m, 8H), 7.52 (s, 2H). ^{13}C NMR (600 MHz, $CDCl_3$): δ 9.50, 15.69, 16.72, 63.78, 119.94, 125.72, 126.56, 127.04, 131.79, 134.73, 135.08, 135.25, 139.96, 151.42, 161.27. FT-IR (ATR): 1699 cm^{-1} (s), νC═O; 1610 cm^{-1} (m), νC═N. Anal. calcd for $C_{76}H_{72}N_8O_8Zn_2$: C, 67.31; H, 5.35. 8.26. Found: C, 67.48; H, 5.33; N, 8.23. λ_{max}: 367 nm (51 700 M^{-1}cm^{-11}/Zn_2; 25 800 M^{-1} cm^{-1}/Zn). HRMS (ESI+) calculated for $C_{76}H_{73}N_8O_8Zn_2$ ([M + H]$^+$): m/z 1355.4135. Found: 1355.4153. CCDC 1983238.

Synthesis of $Cu_2(L^1)_2$. H_2L^1 (0.100 g, 0.164 mmol) was dissolved in 21 mL of a 20:1 THF/MeOH (v/v) solution in a 50 mL round-bottom flask at room temperature and stirred. $Cu(OAc)_2\cdot H_2O$ (0.039 g, 0.197 mmol, 1.2 equiv) was added as a solid, causing a color change from bright yellow to deep orange-brown. The flask was loosely capped and stirred at room temperature for 2 h before being reduced to a concentrate using a rotary evaporator, then stored at 0 °C overnight. The complex was collected as a bronze powder by vacuum filtration (yield: 0.103 g, 93%). FT-IR (ATR): 1701 cm^{-1} (s), νC═O. Anal. calcd for $C_{76}H_{72}N_8O_8Cu_2$: C, 67.49; H, 5.37; 8.28. Found: C, 67.33; H, 5.26; N, 8.21. λ_{max}: 394 nm (66 200 M^{-1} cm^{-1}/Cu_2; 33 100 M^{-1} cm^{-1}/Cu). HRMS (ESI+) calculated for $C_{76}H_{73}N_8O_8Cu_2$ ([M + H]$^+$): m/z 1354.4116. Found: 1354.4113. CCDC 1936510.

Synthesis of $UO_2(L^1)$. H_2L^1 (0.100 g, 0.164 mmol) was dissolved in 21 mL of a 20:1 THF/MeOH (v/v) solution in a 50 mL round-bottom flask at room temperature and stirred. $UO_2(OAc)_2\cdot 2H_2O$ (0.083 g, 0.197 mmol, 1.2 equiv) was added as a solid, causing a gradual color change from bright yellow to deep red-brown. The flask was loosely capped and stirred at room temperature for 3 h before being reduced to a concentrate using a rotary evaporator. The solution was then stored at 0 °C overnight. The complex was collected as an orange-brown crystalline powder by vacuum filtration (Yield: 0.098 g, 68%). ^{1}H NMR (400 MHz, $CDCl_3$): δ 1.38 (t, J = 7.60 Hz, 6H), 2.52 (s, 6H), 2.93 (q, J = 7.63 Hz, 4H), 5.89 (s, 4H), 7.36−7.43 (m, 8H), 7.62 (m, 4H), 7.87 (m, 2H), 9.88 (s, 2H). ^{13}C NMR (600 MHz, $CDCl_3$): δ 10.09, 17.01, 18.61, 68.42, 117.19, 126.24, 127.82, 128.48, 128.63, 128.87, 135.85, 136.06, 137.67, 143.57, 145.43, 154.81, 172.66. FT-IR (ATR): 1389 cm^{-1} (m), νC‴O; 908 cm^{-1} (s), ν_3O═U═O (s). Anal. calcd for $C_{38}H_{37}N_4O_6U$: C, 51.64; H, 4.22; N, 6.34. Found: C, 51.84; H, 4.23; N, 6.34. λ_{max}: 386 nm (41 600 M^{-1} cm^{-1}). HRMS (ESI+) calculated for $C_{38}H_{37}N_4O_6U$ ([M + H]$^+$): m/z 883.2111. Found: 883.3192. CCDC 1936509.

Synthesis of $UO_2(L^2)$. To a solution containing H_2L^2 (0.0500 g, 0.0778 mmol) in 5 mL of 9:1 THF/MeOH (v/v), $UO_2(OAc)_2\cdot 2H_2O$ (0.0330 mg, 0.0778 mmol) was added as a solid. The capped solution was left to stir at room temperature overnight (approximately 12 h). The solution was then concentrated by means of a rotary evaporator and subsequently chilled in a freezer for 48 h to induce crystallization. The product was collected via vacuum filtration and washed in ether (24 mg, 34%). ^{1}H NMR (600 MHz, $CDCl_3$): δ 1.37 (t, J = 6.66 Hz, 6H), 2.43 (s, 6H), 2.51 (s, 6H), 2.92 (q, J = 6.43 Hz, 4H), 5.88 (s, 4H), 7.35−7.39 (m, 6H), 7.60 (m, 6H), 9.81 (s, 2H). ^{13}C NMR (600 MHz, $CDCl_3$): δ 10.12, 17.04, 18.61, 20.25, 68.31, 117.73, 126.14, 128.48, 128.57, 128.85, 135.44, 135.96, 136.83, 137.15, 143.27, 143.71, 153.85, 172.59. FT-IR (ATR): 1390 cm^{-1} (m), νC‴O; 918 cm^{-1} (s), ν_3O═U═O (s). Anal. calcd for $C_{40}H_{40}N_4O_6U$: C, 52.75; H, 4.43; N, 6.15. Found: C, 52.67; H, 4.47; N, 6.19. λ_{max}: 388 nm (55 000 M^{-1} cm^{-1}) HRMS (ESI+) calculated for $C_{40}H_{40}N_4O_6NaU$ ([M + Na]$^+$): m/z 933.3353. Found: 933.3431. CCDC 1971927.

RESULTS AND DISCUSSION

The pyrrophen ligands $\mathbf{H_2L^1}$ and $\mathbf{H_2L^2}$ were prepared through the condensation of the respective o-phenylenediamines with benzyl 4-ethyl-5-formyl-3-methyl-1H-pyrrole-2-carboxylate (**3**) (Scheme 2) in methanol at room temperature. The resulting products were found to precipitate from solution as bright

https://dx.doi.org/10.1021/acs.inorgchem.0c00439
Inorg. Chem. XXXX, XXX, XXX−XXX

Scheme 2. Synthesis of Pyrrophen Ligands

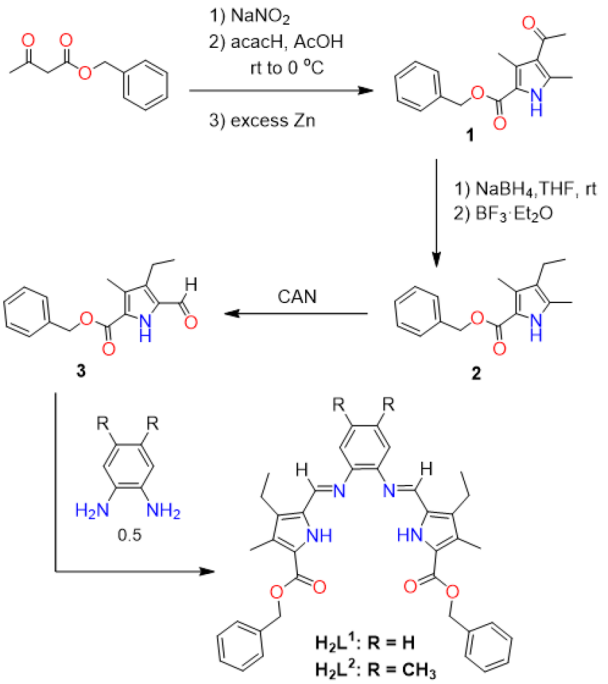

yellow solids. The synthesis of compound **3** is achieved with the regiospecific oxidation of a 5-methyl pyrrole using cerium(IV) ammonium nitrate.[33,34] Single crystals of $\mathbf{H_2L^1}$ and $\mathbf{H_2L^2}$ suitable for X-ray diffraction were grown by slow diffusion (CH_2Cl_2/CH_3OH). In the solid-state, both the $\mathbf{H_2L^1}$ and $\mathbf{H_2L^2}$ free ligands were found to adopt slightly cupped conformations and form adducts with neutral solvent molecules (methanol; Figure 1) through pyrrolic hydrogen-

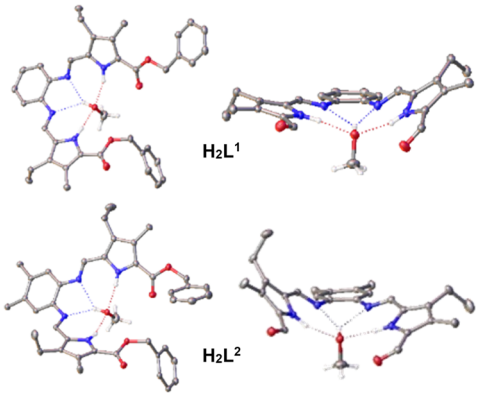

Figure 1. Left: structures of $\mathbf{H_2L^1{\cdot}CH_3OH}$ (top) and $\mathbf{H_2L^2{\cdot}CH_3OH}$ (bottom), grown from CH_2Cl_2/CH_3OH and CH_3OH, respectively. Right: side-on views of $\mathbf{H_2L^1{\cdot}CH_3OH}$ and $\mathbf{H_2L^2{\cdot}CH_3OH}$ along coordination plane (right) showing solvent interactions. H atoms and substituents (right) partially removed for clarity. Ellipsoids at 50%.

bonding. Such interactions have been observed previously in macrocyclic calix[4]pyrrole species[35,36] as well as for Schiff base expanded porphyrins.[13] Both ligands were found to have donor–acceptor distances that compare well with those of their macrocyclic cousins, though they more strongly resemble those of the Schiff base expanded porphyrins (Table 1). The diffuse nature of the N_{pyr}—H bond that predisposes it to these interactions is also apparent in the solution state by ^{1}H

Table 1. Average Bond Lengths (Å)[a] for Hydrogen Bonds and Methanol for Pyrrophen Ligands and Adducts from References 13 and 35

bond	H_2L^1	H_2L^2	ref 13	ref 35
HO···N_{im}	2.937	2.918	2.891	
OH···N_{im}	(2.24)	(2.20)	(2.09)	
O–H	*0.84*	*0.84*	*0.95*	*nr*
N···OH	2.844	2.827	2.853	3.155
NH···OH	(1.96)	(1.98)	(1.97)	(2.33)
N–H	*0.91*	*0.86*	*0.89*	*0.90*
H_3C–OH	1.43	1.41	1.41	1.29

[a]Lengths with unabridged significant figures and ESD values can be found in the Supporting Information. (nr) Not reported.

NMR—the pyrrole H atoms are observed downfield at 9.70 ppm ($\mathbf{H_2L^1}$) and 10.25 ppm ($\mathbf{H_2L^2}$) as broad resonances, indicating considerable hydrogen delocalization (Figures S1 and S5). These similarities to macrocyclic species not only are of note for their reported correlation in anion binding[37] but give the pyrrophen framework a prospective amphoteric coordination module for insight into self-assembly and molecular recognition of other species.

Complexes were prepared by adding 1.2 equiv of $M(OAc)_2$ (M = Cu, Zn, UO_2) into a THF/MeOH (20:1, v/v) solution of $\mathbf{H_2L^1}$ or $\mathbf{H_2L^2}$. Upon addition of the metal acetate, each solution featured a distinct color change from yellow to brown, orange, or deep red for the copper, zinc, and uranyl complexes, respectively. Intensely colored solids were isolated by filtration after concentrating the solution under reduced pressure and cooling to 0 °C. Single crystals of the copper, zinc, and uranyl complexes of $\mathbf{H_2L^1}$ and the uranyl complex of $\mathbf{H_2L^2}$ were grown from CH_2Cl_2/CH_3OH and characterized by X-ray diffraction. Unsurprisingly, the copper and zinc pyrrophen complexes form M_2L_2 helicate ensembles (Figure 2)

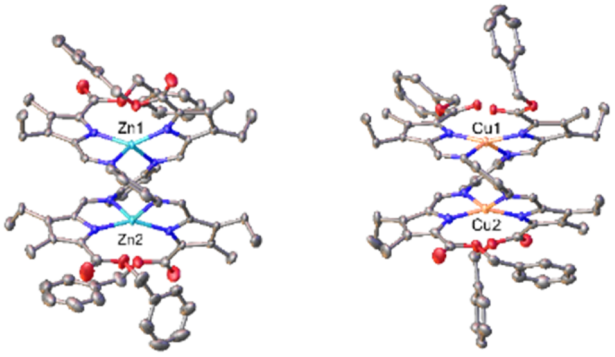

Figure 2. Structures of $\mathbf{Zn_2(L^1)_2}$ (left) and $\mathbf{Cu_2(L^1)_2}$ (right) viewed along planes of phenyl spacers. Ellispsoids at 50%. Hydrogen atoms removed for clarity.

comparable to those previously reported by Wu and Yang,[21,26] whereas the uranyl complexes adopt the hexagonal bipyramidal geometry (Figure 3) seen in porphyrin-type macrocyclic complexes (Scheme 1).[38] To our knowledge, there is only one other reported structure in which the equatorial plane of uranyl is satisfied completely by a single, softer-donor, nonmacrocyclic ligand—a bipodal aroylthiourea-substituted bipyridine ligand (N_4S_2).[39] Recently, chelation of uranyl by a harder, catecholamine-based ligand was also reported, but no structures were presented.[40] $\mathbf{UO_2(L^1)}$ and

https://dx.doi.org/10.1021/acs.inorgchem.0c00439
Inorg. Chem. XXXX, XXX, XXX–XXX

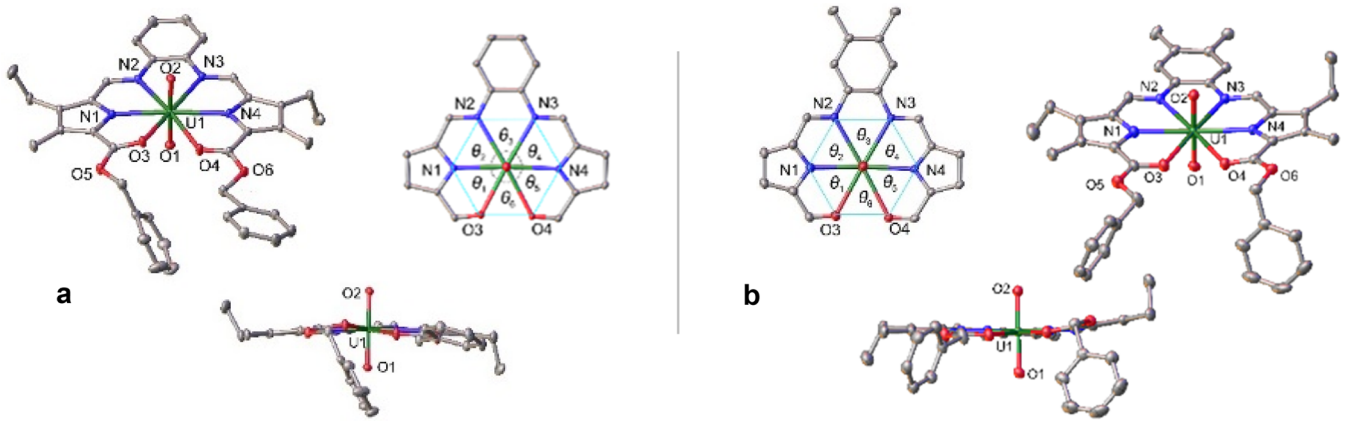

Figure 3. Structures of $UO_2(L^1)$ (a) and $UO^2(L^2)$ (b) showing full structure, views down the O═U═O units, and the equatorial planes. Hydrogen atoms and/or substituents removed for clarity. Ellipsoids at 50%. (a) θ_1, 60.96(5)°; θ_2, 61.35(6)°; θ_3, 60.71(5)°; θ_4, 61.91(6)°; θ_5, 60.06(5)°; θ_6, 55.92(5)°; θ_{avg}, 60.15(5)°; $\sum\theta$ = 360.1°. (b) θ_1, 60.19(8)°; θ_2, 61.41(8)°; θ_3, 60.25(7)°; θ_4, 62.05(8)°; θ_5, 60.04(7)°; θ_6, 56.20(7)°; θ_{avg}, 60.19(8)°; $\sum\theta$ = 360.14°.

Table 2. Selected Bond Lengths (Å) for Pyrrophen Ligands and Their Complexes

	H_2L^1	H_2L^2	$Zn_2L_2^1$	$Cu_2L_2^1$	$UO_2(L^1)$	$UO_2(L^2)$
C═N_{im}	1.2839(19)	1.2816(14)	1.3075(13)	1.299(3)	1.302(2)	1.302(4)
C═O_{ester}	1.2134(19)	1.2132(13)	1.2085(14)	1.209(3)	1.237(2)	1.235(4)
M−N_{im}			2.0793(9)	2.048(2)	2.6597(17)	2.664(2)
M−N_{pyr}			1.9592(9)	1.933(2)	2.4374(16)	2.441(3)
M−O					2.5789(14)	2.673(2)
U═O_{yl}					1.7722(16)	1.774(2)

$UO_2(L^2)$ represent unique complexes in this regard, and highlight the potential the pyrrophen system shows for molecular recognition of uranyl by completely satisfying the equatorial plane. Selected bond lengths for all complexes as well as the free ligands are summarized in Table 2.

Notably, the formation of the double-stranded dinuclear copper and zinc complexes indicates that the binding pocket of the pyrrophen system cannot satisfy the coordination sphere of these late transition metals in a 1:1 binding motif, and instead the ligand twists about the phenyl spacer to form a ditopic system in the observed 2:2 fashion. The zinc and copper centers adopt distorted tetrahedral geometries with average Cu−N_{pyr}, Cu−N_{im}, Zn−N_{pyr}, and Zn−N_{im} bond lengths of 1.993(2) Å, 2.048(2) Å, 1.9592(9) Å, and 2.0793(9) Å, respectively. The metal centers lie 3.300 Å (Cu) and 3.667 Å (Zn) apart. The formation of this helicate can also be observed for the zinc complex in solution via ^{1}H NMR as the ligand's methylene protons (δ 5.29) split into two distinct diastereotopic peaks (δ 5.20, d; 4.27, d), signifying axial chirality (Figures S2 and S3).[21]

While Zn^{2+} and Cu^{2+} undergo self-assembly into 2:2 helicate complexes in the presence of H_2L^1, the distinct steric demands of the uranyl ion render complexes with a 1:1 configuration in which L^1 and L^2 fully occupy the equatorial plane as hexadentate ligands. This is evident in both solution and the solid state. ^{1}H NMR of the uranyl complexes shows single enantiotopic signals for the benzylic methylene protons (ca. 5.8 ppm). The hexagonal bipyramidal uranyl complexes are undoubtably U(VI) species, evidenced by average U═O_{yl} bond lengths of 1.7722(16) Å ($UO_2(L^1)$) and 1.774(2) Å ($UO_2(L^2)$).[41] Notably, the average C═O distances of 1.236(3) Å unambiguously represent a coordinative interaction of the carbonyl oxygen with uranium in both cases. The corresponding average C═O distance in the "free" ester carbonyls for $Cu_2(L^1)_2$ and $Zn_2(L^1)_2$ is 1.209(3) Å and 1.2084(14). The average U−N_{im} lengths of both complexes (Table 2) are approximately 0.15 Å longer than those usually found for U(VI) salophen species[42] and are on par with U−N_{im} lengths reported for expanded porphyrin complexes, as are the average U−N_{pyr} lengths,[11] though these distances do differ somewhat from those of a comparable macrocyclic uranyl grandephyrin complex[13] which features a slightly larger pocket—the U−N_{im} and U_{Npyr} lengths of the pyrrophen species are nearly 0.20 and 0.10 Å shorter, respectively. It is noted for the grandephryin complex that the uranyl cation is shifted off-center away from the imine N atoms—the uranium center lies 2.536 Å from the midpoint of the vector defined by the imine N atoms and 2.265 Å from the vector defined by the meso-bridged pyrrole N atoms,[13] whereas the pyrrophen complexes are significantly more centered with the uranium atom lying an average of 2.299 Å from the imine midpoint and 2.318 Å from the midpoint of the vector defined by the carbonyl O atoms. The near linearity of the pyrrole donors for $UO_2(L^1)$ and $UO_2(L^1)$ (N_1−U−N_4 = 175.61(6)° and 174.99(9)°, respectively) as well as the average angle between donors and $\sum\theta$ values (60.15(6)°, 360.91°, and 60.02(8)°, 360.14°, respectively) also reflect that the uranyl resides almost perfectly in the center of the ligand's pocket, similar to some macrocyclic systems, as well as highlights the planarity of these complexes, a feature which is uncommon among the typically ruffled macrocyclic complexes[13−15] (Figure 3). This illustrates the ability of uranyl to engage favorably in primarily covalent interactions, as the deprotonated pyrrole N atoms possess low ionic character. Additionally, the high planarity and subsequent retention of conjugation of L^1 when complexed to uranyl allow

https://dx.doi.org/10.1021/acs.inorgchem.0c00439
Inorg. Chem. XXXX, XXX, XXX−XXX

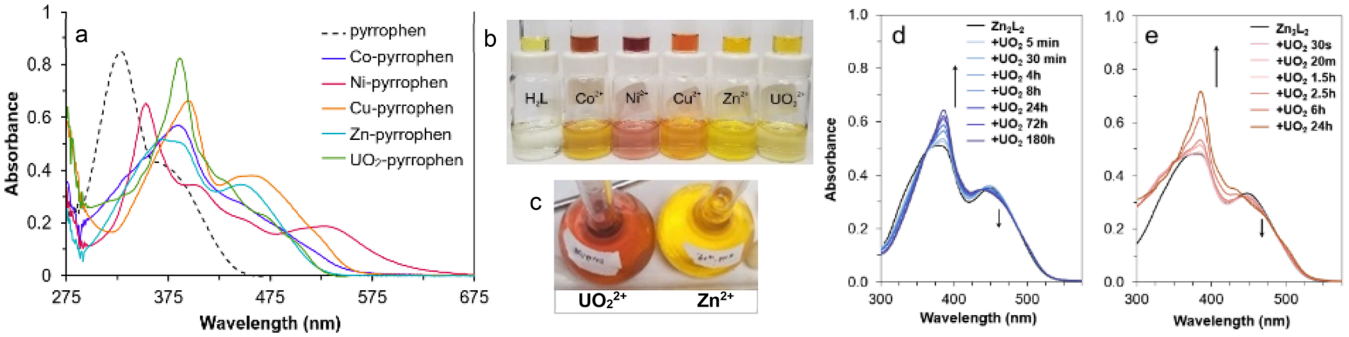

Figure 4. (a) UV−vis spectra of $\mathbf{H_2L^1}$ and complexes in 9:1 THF/MeOH (v/v). Data shown are final traces of the titration of 20 μM $\mathbf{H_2L^1}$ with M^{2+} to form 1:1 or 2:2 complexes. (b) 500 μM (upper vials) and 50 μM (lower vials) colorimetric series of $\mathbf{H_2L^1}$ and complexes in 9:1 THF/MeOH (v/v), (c) top-down views of $\mathbf{UO_2(L^1)}$ (right) and $\mathbf{Zn_2(L^1)_2}$ (left) solutions, 500 μM in CH_3CN. (d and e) Addition of 0.5 (d) and 1.0 (e) equivalent UO_2^{2+} (per Zn^{2+}) to $\mathbf{Zn_2(L^1)_2}$, 10 μM in 9:1 THF/MeOH.

for significant delocalization of charge throughout the π-system, thereby further "softening" the pyrroles.

While these species are interesting for their unique structures in the solid-state, the solution state behavior of pyrrophen is also worth investigation, as the structural features of the uranyl complexes suggest that the pyrrophen system is particularly well-suited for forming stable uranyl complexes. Given the spontaneous assembly of each metal complex at room temperature and without the addition of base, as well as the marked color differences among them, there is the potential of this system to be exploited in further studies for molecular recognition of UO_2^{2+}. Initial screening of a wide array of metal acetates (Mg^{2+}, Ca^{2+}, VO^{2+}, Mn^{2+}, Fe^{2+} Fe^{3+}, Co^{2+}, Ni^{2+}, Cu^{2+}, Zn^{2+}, Ce^{3+}, Ce^{4+}, Dy^{3+}, Th^{4+}, and UO_2^{2+}) was conducted to determine the range of coordinating cations for $\mathbf{H_2L^1}$. As determined by UV−vis spectroscopy, only Co^{2+}, Ni^{2+}, Cu^{2+}, Zn^{2+}, and UO_2^{2+} were found to form metal complexes under ambient conditions. No other ions were observed to induce a visible change to pyrrophen. The ligand ($\mathbf{H_2L^1}$) features an intense $\pi \rightarrow \pi^*$ band (Soret-like) at 328 nm (ε = 42 800 M^{-1} cm^{-1}) with a shoulder at 375 nm ($\varepsilon \approx$ 22 000 M^{-1} cm^{-1}) indicative of charge-transfer from a coordinating solvent molecule (as seen in the solid-state). Similar features are observed for $\mathbf{H_2L^2}$ (λ_{max} = 319 nm, ε = 49, 100 M^{-1} cm^{-1}; Figure S14). Coordination of to Co^{2+}, Ni^{2+}, Cu^{2+}, Zn^{2+}, or UO_2^{2+} results in a substantial bathochromic shift of the $\pi \rightarrow \pi^*$ band (Figure 4). Only coordination to UO_2^{2+} results in retention of approximately the same ε, or an increase in ε (41 600 M^{-1} cm^{-1} for $\mathbf{UO_2(L^1)}$; 55 000 for $\mathbf{UO_2(L^2)}$) as the free ligand, indicating the uranyl complexes are planar in solution, whereas the transition metal complexes are not. This behavior is also distinct from expanded porphyrin analogues, which either show a marked increase or decrease in ε due to ruffling or bowing of the ligand on complexation.[6,14] UV−vis titrations of metal acetates into a solutions of pyrrophen ($\mathbf{H_2L^1}$) show clear isosbestic points and confirm 1:1 binding ratios for all complexes (1:1 or 2:2), but the presence of multiple isosbestic points in the nickel titration data, and the smaller bathochromic shift of the $\pi \rightarrow \pi^*$ band suggest structural features distinct from that of the other transition metal species (Figure S19). Titrations of $\mathbf{H_2L^1}$ with acetic acid resulted in no spectroscopic changes, affirming complex formation is not hindered by ligand−acetate interactions. Most of the transition metal complexes feature a λ_{max} in a similar range (approximately 370−390 nm) as that of the uranyl complex, except for nickel (λ_{max} = 352), but their lower-energy absorptions are more intense, leading to visible color differences in solution (Figure 4a,b). The uranyl and zinc complexes are the most similar in color when viewed side on; however, when viewed from above, the $\mathbf{UO_2(L^1)}$ solution is distinctly red-orange in color (Figure 4b,c). While the visible color differences alone are not sufficient to clearly distinguish the uranyl solution from the others, this can be done so spectroscopically, as $\mathbf{UO_2(L^1)}$ is the only species with a sharp, intense absorption at 386 nm; however, greater differentiation both in terms of solution color and absorption profile are still necessary. These features are not ideal, but they are a promising starting point in terms of molecular recognition of uranyl. Additionally, it should be noted that colorimetric differences, though useful from an identification standpoint, do not speak to the ability of this ligand to selectively bind uranyl from a mixture. Thus, further qualitative studies to determine the binding preferences of pyrrophen were conducted in which the ability of UO_2^{2+} to displace zinc or copper from the M_2L_2 complexes was investigated.

Replacement of cobalt and nickel was not pursued, as the cobalt complex is observed to dissociate rather quickly after formation, even in an excess of Co^{2+} (Figure S26), and both the cobalt and nickel complexes are colorimetrically distinct from the uranyl complex in solution (Figure 4a−c). On addition of UO_2^{2+} to solutions of $\mathbf{Zn_2(L^1)_2}$, displacement of Zn^{2+} was observed using UV−vis spectroscopy via the immediate growth of the characteristic $\mathbf{UO_2(L^1)}$ absorption features (Figure 4d,e). Even when 0.5 per-metal equivalents of UO_2^{2+} was introduced, this replacement was observed within minutes. The same experiments were conducted using $\mathbf{Cu_2(L^1)_2}$, but formation of the uranyl complex was not observed, indicating the copper helicate is more stable in solution. From these studies, we have determined that the stability of the monomeric $\mathbf{UO_2(L^1)}$ complex is intermediate to that of the ditopic $\mathbf{Cu_2(L^1)_2}$ and $\mathbf{Zn_2(L^1)_2}$ helicates, though this may not necessarily reflect the stabilities of exclusively 1:1 species.

In an attempt to characterize this quantitatively, formation constants were calculated for complexes of $\mathbf{H_2L^1}$ (Table S2) using UV−vis titration data,[31,43,44] though it must be acknowledged that the methods used are based on the assumption that 1:1 complexes are being formed, not the 2:2 complexes which are known to self-assemble in the presence of Zn^{2+} or Cu^{2+}.[21,26] Where higher order supramolecular self-assembly is concerned, such studies are nontrivial and require a clear mechanism of formation and independent treatment of

https://dx.doi.org/10.1021/acs.inorgchem.0c00439
Inorg. Chem. XXXX, XXX, XXX−XXX

intra- and intermolecular constants.[43,45] Approximations of the binding constants for 1:1 complexes in 9:1 THF/MeOH are a reasonable benchmark for comparing the *relative* binding affinity of $\mathbf{H_2L^1}$ for transition metal ions[31,44] and should always be secondary to more detailed qualitative studies. These approximated log β_{11} values (Co^{2+}, 6.11 ± 0.71; Ni^{2+}, 7.31 ± 0.53; Cu^{2+}, 6.02 ± 1.33; Zn^{2+}, 5.27 ± 0.09; UO_2^{2+}, 6.74 ± 0.80) suggest that the copper complex should be more stable than the zinc complex. This is consistent with what is observed experimentally for the prepared 2:2 complexes with respect to replacement by uranyl; however, this is difficult to conclude given the nontraditional solvent system. The cobalt complex is observed to fall apart after formation, yet the calculated log β_{11} is higher than other stable complexes, and the log β_{11} for $\mathbf{UO_2(L^1)}$ is calculated to be higher than that of the 1:1 copper complex. Additionally, formation of the uranyl complex at concentrations appropriate for UV−vis spectroscopy is significantly slower than that of the transition metal species, which further complicates analysis (Figure S23), however the presence of methyl groups on the backbone of $\mathbf{H_2L^2}$ appears to improve the kinetics considerably (Figure S24). The formation constant for $\mathbf{UO_2(L^1)}$ cannot be reasonably compared to those of other reported aqueous-soluble systems[40,46] but is greater than those reported for macrocyclic systems in mixed organic solvents, reflecting the value of a well-sized and flexible binding pocket.[47,48] (Further information is given in the Supporting Information.)

In conclusion, pyrrophen, a sal-porphyrin analogue, as well as its dimethyl derivative have been prepared and characterized in the solution and solid state via NMR and UV−vis spectroscopy, and with single crystal X-ray diffraction, as have the complexes $\mathbf{Cu_2(L^1)_2}$, $\mathbf{Zn_2(L^1)_2}$, $\mathbf{UO_2(L^1)}$, and $\mathbf{UO_2(L^2)}$. Of note is the coordination of the free ligands to methanol, thereby showing the inherent lack of electronegativity on the pyrrole moieties and preferred pseudoplanar orientation, as observed in calix[4]pyrrole systems.[37] Structural analyses of the UO_2^{2+} complexes suggest this ligand is especially well-suited for uranyl coordination and help to further elucidate the covalent-type coordination behavior of the uranyl cation. $\mathbf{H_2L^1}$ was found to preferentially bind UO_2^{2+} over Zn^{2+} but not over Cu^{2+}—the ability of uranyl to displace zinc from the helicate architecture is of note, as these are the two most similarly colored complexes. From a colorimetric identification perspective, this is valuable in that it reduces the possibility of false-positive responses for uranyl. The selectivity of this ligand system for uranyl still requires improvement in order to avoid competition from ions such as Cu^{2+} and Ni^{2+} and to be able to identify UO_2^{2+} from a mixture of such ions, but features such as its synthetic accessibility and tunability, as well as its utilitarian hexadentate cavity, make it an ideal framework for such endeavors. This ligand and its complexes give insight into the potential of softer-donor acyclic systems as suitable candidates for selective uranyl recognition or extraction by taking advantage of uranyl's proposed covalent f orbitals.[8,49] With uranyl forming the only planar complex of the cations and given the synthetic modularity of the ligand, it is feasible to prepare a pyrrophen derivative that sterically disfavors the formation of transition metal helicate complexes—this is a potential route by which to more clearly study the solution phase thermodynamics without needing to consider the self-assembly of higher order complexes as a complicating factor. Future work will also include the preparation of water-soluble derivatives as such data are most relevant in aqueous systems and would be best for comparison with other systems. Despite the limitations we have encountered in quantitatively describing the binding preferences of this system, we are encouraged by the narrow range of cations which pyrrophen can coordinate, as our preliminary investigations demonstrate it has no affinity for Ln^{3+} ions or Th^{4+} under ambient conditions—exclusion of these species is valuable with respect to applications for environmental cleanup or nuclear waste remediation. Studies focused on the selective coordination of uranyl are ongoing, with modifications to improve binding kinetics, sensitivity, selectivity, and colorimetric response being pursued. This (along with the work from Abram et al.[39]) warrants further investigation into the potential use of this highly modular and chromatic framework in selective actinyl recognition.

■ ASSOCIATED CONTENT

Supporting Information

The Supporting Information is available free of charge at https://pubs.acs.org/doi/10.1021/acs.inorgchem.0c00439.

NMR, UV−vis, and other solution-state data including additional commentary on binding constants, as well as crystallographic information (PDF)

Accession Codes

CCDC 1936495, 1936509−1936510, 1971893, 1971927, and 1983238 contain the supplementary crystallographic data for this paper. These data can be obtained free of charge via www.ccdc.cam.ac.uk/data_request/cif, or by emailing data_request@ccdc.cam.ac.uk, or by contacting The Cambridge Crystallographic Data Centre, 12 Union Road, Cambridge CB2 1EZ, UK; fax: +44 1223 336033.

■ AUTHOR INFORMATION

Corresponding Author

Anne E. V. Gorden − *Auburn University, Department of Chemistry and Biochemistry, Auburn, Alabama 36849, United States;* orcid.org/0000-0001-6623-9880; Email: anne.gorden@auburn.edu

Authors

Jacob T. Mayhugh − *Auburn University, Department of Chemistry and Biochemistry, Auburn, Alabama 36849, United States*

Julie E. Niklas − *Auburn University, Department of Chemistry and Biochemistry, Auburn, Alabama 36849, United States*

Madeleine G. Forbes − *Auburn University, Department of Chemistry and Biochemistry, Auburn, Alabama 36849, United States*

John D. Gorden − *Auburn University, Department of Chemistry and Biochemistry, Auburn, Alabama 36849, United States;* orcid.org/0000-0002-0304-1954

Complete contact information is available at: https://pubs.acs.org/10.1021/acs.inorgchem.0c00439

Author Contributions

‡These authors contributed equally. The manuscript was written through contributions of all authors. All authors have given approval to the final version of the manuscript.

Funding

United States Department of Energy - Chemical Sciences, Geosciences, and Biosciences (CSGB) subdivision for Heavy Elements Chemistry

Notes

The authors declare no competing financial interest.

■ ACKNOWLEDGMENTS

The authors would like to acknowledge that this work was funded by the United States Department of Energy − Basic Energy Sciences through the Chemical Sciences, Geosciences, and Biosciences (CSGB) subdivision for Heavy Elements Chemistry with Award DE-SC0019177 to Auburn University.

■ REFERENCES

(1) Pearson, R. G. Hard and soft acids and bases, HSAB, part 1: Fundamental principles. *J. Chem. Educ.* **1968**, *45* (9), 581.
(2) Takao, K.; Akashi, S. Exploring the catalytic activity of Lewis-acidic uranyl complexes in the nucleophilic acyl substitution of acid anhydrides. *RSC Adv.* **2017**, *7* (20), 12201−12207.
(3) Thuéry, P.; Harrowfield, J. Uranyl Ion Complexes with trans-3-(3-Pyridyl)acrylic Acid Including a Uranyl−Copper(II) Heterometallic Framework. *Eur. J. Inorg. Chem.* **2014**, *2014* (28), 4772−4778.
(4) DeVore, M. A., II; Kerns, S. A.; Gorden, A. E. V. Characterization of Quinoxolinol Salen Ligands as Selective Ligands for Chemosensors for Uranium. *Eur. J. Inorg. Chem.* **2015**, *2015* (34), 5708−5714.
(5) Jeazet, H. B. T.; Gloe, K.; Doert, T.; Mizera, J.; Kataeva, O. N.; Tsushima, S.; Bernhard, G.; Weigand, J. J.; Lindoy, L. F.; Gloe, K. Uranyl(VI) binding by bis(2-hydroxyaryl)diimine and bis(2-hydroxyaryl)diamine ligand derivatives. Synthetic, X-ray, DFT and solvent extraction studies. *Polyhedron* **2016**, *103*, 198−205.
(6) Sessler, J. L.; Seidel, D.; Vivian, A. E.; Lynch, V.; Scott, B. L.; Keogh, D. W. Hexaphyrin(1.0.1.0.0.0): An Expanded Porphyrin Ligand for the Actinide Cations Uranyl (UO22+) and Neptunyl (NpO2+). *Angew. Chem., Int. Ed.* **2001**, *40* (3), 591−594.
(7) Brewster, J. T.; He, Q.; Anguera, G.; Moore, M. D.; Ke, X.-S.; Lynch, V. M.; Sessler, J. L. Synthesis and characterization of a dipyriamethyrin−uranyl complex. *Chem. Commun.* **2017**, *53* (36), 4981−4984.
(8) Baker, R. J. New Reactivity of the Uranyl(VI) Ion. *Chem. - Eur. J.* **2012**, *18* (51), 16258−16271.
(9) Andrews, M. B.; Cahill, C. L. Uranyl Bearing Hybrid Materials: Synthesis, Speciation, and Solid-State Structures. *Chem. Rev.* **2013**, *113* (2), 1121−1136.
(10) Hudson, M. J.; Harwood, L. M.; Laventine, D. M.; Lewis, F. W. Use of Soft Heterocyclic N-Donor Ligands To Separate Actinides and Lanthanides. *Inorg. Chem.* **2013**, *52* (7), 3414−3428.
(11) Sessler, J. L.; Vivian, A. E.; Seidel, D.; Burrell, A. K.; Hoehner, M.; Mody, T. D.; Gebauer, A.; Weghorn, S. J.; Lynch, V. Actinide expanded porphyrin complexes. *Coord. Chem. Rev.* **2001**, *216−217*, 411−434.
(12) Sessler, J. L.; Melfi, P. J.; Seidel, D.; Gorden, A. E. V.; Ford, D. K.; Palmer, P. D.; Tait, C. D. Hexaphyrin(1.0.1.0.0.0). A new colorimetric actinide sensor. *Tetrahedron* **2004**, *60* (49), 11089−11097.
(13) Sessler, J. L.; Gorden, A. E. V.; Seidel, D.; Hannah, S.; Lynch, V.; Gordon, P. L.; Donohoe, R. J.; Drew Tait, C.; Webster Keogh, D. Characterization of the interactions between neptunyl and plutonyl cations and expanded porphyrins. *Inorg. Chim. Acta* **2002**, *341*, 54−70.
(14) Brewster, J. T., 2nd; Mangel, D. N.; Gaunt, A. J.; Saunders, D. P.; Zafar, H.; Lynch, V. M.; Boreen, M. A.; Garner, M. E.; Goodwin, C. A. P.; Settineri, N. S.; Arnold, J.; Sessler, J. L. In-Plane Thorium(IV), Uranium(IV), and Neptunium(IV) Expanded Porphyrin Complexes. *J. Am. Chem. Soc.* **2019**, *141* (44), 17867−17874.
(15) Brewster, J. T.; Zafar, H.; Root, H. D.; Thiabaud, G. D.; Sessler, J. L. Porphyrinoid f-Element Complexes. *Inorg. Chem.* **2020**, *59* (1), 32−47.
(16) Rambo, B. M.; Sessler, J. L. Oligopyrrole Macrocycles: Receptors and Chemosensors for Potentially Hazardous Materials. *Chem. - Eur. J.* **2011**, *17* (18), 4946−4959.
(17) Zheng, X.-J.; Bell, N. L.; Stevens, C. J.; Zhong, Y.-X.; Schreckenbach, G.; Arnold, P. L.; Love, J. B.; Pan, Q.-J. Relativistic DFT and experimental studies of mono- and bis-actinyl complexes of an expanded Schiff-base polypyrrole macrocycle. *Dalton Transactions* **2016**, *45* (40), 15910−15921.
(18) Arnold, P. L.; Jones, G. M.; Pan, Q.-J.; Schreckenbach, G.; Love, J. B. Co-linear, double-uranyl coordination by an expanded Schiff-base polypyrrole macrocycle. *Dalton Transactions* **2012**, *41* (22), 6595−6597.
(19) Love, J. B. A macrocyclic approach to transition metal and uranyl Pacman complexes. *Chem. Commun.* **2009**, No. 22, 3154−3165.
(20) DeVore, M. A., II; Kerns, S. A.; Gorden, A. E. V. Characterization of Quinoxolinol Salen Ligands as Selective Ligands for Chemosensors for Uranium. *Eur. J. Inorg. Chem.* **2015**, *2015* (34), 5708−5714.
(21) Wu, Z.; Chen, Q.; Xiong, S.; Xin, B.; Zhao, Z.; Jiang, L.; Ma, J. S. Double-Stranded Helicates, Triangles, and Squares Formed by the Self-Assembly of Pyrrol-2-ylmethyleneamines and ZnII Ions. *Angew. Chem., Int. Ed.* **2003**, *42* (28), 3271−3274.
(22) Bhowon, M. G.; Li Kam Wah, H.; Dosieah, A.; Ridana, M.; Ramalingum, O.; Lacour, D. Synthesis, Characterization, and Catalytic Activity of Metal Schiff Base Complexes Derived from Pyrrole-2-carboxaldehyde. *Synth. React. Inorg. Met.-Org. Chem.* **2004**, *34* (1), 1−16.
(23) Maeda, H. Supramolecular Chemistry of Acyclic Oligopyrroles. *Eur. J. Org. Chem.* **2007**, *2007* (32), 5313−5325.
(24) Munro, O. Q.; Joubert, S. D.; Grimmer, C. D. Molecular Recognition: Preorganization of a Bis(pyrrole) Schiff Base Derivative for Tight Dimerization by Hydrogen Bonding. *Chem. - Eur. J.* **2006**, *12* (31), 7987−7999.
(25) Bacchi, A.; Carcelli, M.; Gabba, L.; Ianelli, S.; Pelagatti, P.; Pelizzi, G.; Rogolino, D. Syntheses, characterization and X-ray structure of palladium(II) and nickel(II) complexes of tetradentate pyrrole containing ligands. *Inorg. Chim. Acta* **2003**, *342*, 229−235.
(26) Yang, L.; Chen, Q.; Li, Y.; Xiong, S.; Li, G.; Ma, J. S. Self-Assembly of Bis(pyrrol-2-ylmethyleneamine) Ligands with CuII Controlled by Bridging [−(CH2)n−] Spacers and Weak Intermolecular C−H···Cu Hydrogen Bonding. *Eur. J. Inorg. Chem.* **2004**, *2004* (7), 1478−1487.
(27) Franceschi, F.; Guillemot, G.; Solari, E.; Floriani, C.; Re, N.; Birkedal, H.; Pattison, P. Reduction of Dioxygen by a Dimanganese Unit Bonded Inside a Cavity Provided by a Pyrrole-Based Dinucleating Ligand. *Chem. - Eur. J.* **2001**, *7* (7), 1468−1478.
(28) Reid, S. D.; Blake, A. J.; Wilson, C.; Love, J. B. Syntheses and Structures of Dinuclear Double-Stranded Helicates of Divalent Manganese, Iron, Cobalt, and Zinc. *Inorg. Chem.* **2006**, *45* (2), 636−643.
(29) Xu, H.; Xu, D. C.; Wang, Y. Natural Indices for the Chemical Hardness/Softness of Metal Cations and Ligands. *ACS Omega* **2017**, *2* (10), 7185−7193.
(30) Shannon, R. Revised effective ionic radii and systematic studies of interatomic distances in halides and chalcogenides. *Acta Crystallogr., Sect. A: Cryst. Phys., Diffr., Theor. Gen. Crystallogr.* **1976**, *32* (5), 751−767.
(31) Supramolecular.org | Binding Constant Calculators. http://supramolecular.org.
(32) Awruch, J.; Frydman, B. The total synthesis of biliverdins of biological interest. *Tetrahedron* **1986**, *42* (15), 4137−4146.
(33) Lightner, D. A. An inexpensive, selective procedure for oxidizing alpha-methyl to alpha-formyl pyrroles. *J. Heterocycl. Chem.* **2001**, *38* (5), 1219−1221.
(34) Thyrann, T.; Lightner, D. A. Oxidation of Pyrrole Alpha-Methyl to Formyl with Ceric Ammonium-Nitrate. *Tetrahedron Lett.* **1995**, *36* (25), 4345−4348.
(35) Allen, W. E.; Gale, P. A.; Brown, C. T.; Lynch, V. M.; Sessler, J. L. Binding of Neutral Substrates by Calix[4]pyrroles. *J. Am. Chem. Soc.* **1996**, *118* (49), 12471−12472.

https://dx.doi.org/10.1021/acs.inorgchem.0c00439
Inorg. Chem. XXXX, XXX, XXX−XXX

(36) Sathish Kumar, B.; Panda, P. K. 1D water chain stabilized by meso-expanded calix[4]pyrrole. *CrystEngComm* **2014**, *16* (37), 8669−8672.
(37) Anzenbacher, P.; Jursikova, K.; Lynch, V. M.; Gale, P. A.; Sessler, J. L. Calix[4]pyrroles Containing Deep Cavities and Fixed Walls. Synthesis, Structural Studies, and Anion Binding Properties of the Isomeric Products Derived from the Condensation of p-Hydroxyacetophenone and Pyrrole. *J. Am. Chem. Soc.* **1999**, *121* (47), 11020−11021.
(38) Sessler, J. L.; Vivian, A. E.; Seidel, D.; Burrell, A. K.; Hoehner, M.; Mody, T. D.; Gebauer, A.; Weghorn, S. J.; Lynch, V. Actinide expanded porphyrin complexes. *Coord. Chem. Rev.* **2001**, *216−217*, 411−434.
(39) Noufele, C. N.; Pham, C. T.; Hagenbach, A.; Abram, U. Uranyl Complexes with Aroylbis(N,N-dialkylthioureas). *Inorg. Chem.* **2018**, *57* (19), 12255−12269.
(40) Zhang, Q.; Jin, B.; Zheng, T.; Tang, X.; Guo, Z.; Peng, R. Hexadentate β-Dicarbonyl(bis-catecholamine) Ligands for Efficient Uranyl Cation Decorporation: Thermodynamic and Antioxidant Activity Studies. *Inorg. Chem.* **2019**, *58*, 14626.
(41) Hayton, T. W.; Wu, G. Exploring the Effects of Reduction or Lewis Acid Coordination on the U═O Bond of the Uranyl Moiety. *Inorg. Chem.* **2009**, *48* (7), 3065−3072.
(42) Niklas, J. E.; Hardy, E. E.; Gorden, A. E. V. Solid-state structural elucidation and electrochemical analysis of uranyl naphthylsalophen. *Chem. Commun.* **2018**, *54* (83), 11693−11696.
(43) Thordarson, P. Determining association constants from titration experiments in supramolecular chemistry. *Chem. Soc. Rev.* **2011**, *40* (3), 1305−1323.
(44) Brynn Hibbert, D.; Thordarson, P. The death of the Job plot, transparency, open science and online tools, uncertainty estimation methods and other developments in supramolecular chemistry data analysis. *Chem. Commun.* **2016**, *52* (87), 12792−12805.
(45) Ercolani, G. Assessment of Cooperativity in Self-Assembly. *J. Am. Chem. Soc.* **2003**, *125* (51), 16097−16103.
(46) Vukovic, S.; Hay, B. P.; Bryantsev, V. S. Predicting Stability Constants for Uranyl Complexes Using Density Functional Theory. *Inorg. Chem.* **2015**, *54* (8), 3995−4001.
(47) Rounaghi, G.; Kakhki, R. M. Z. Thermodynamic study of complex formation between dibenzo-18-crown-6 and UO22+ cation in different non-aqueous binary solutions. *J. Inclusion Phenom. Mol. Recognit. Chem.* **2009**, *63* (1), 117.
(48) Rounaghi, G. H.; Nazari, E.; Ghaemi, A.; Mohajeri, M. Complexing ability of a macrocyclic ligand, dibenzo-24-crown-8, with UO22+ in some binary mixed non-aqueous solvents. *J. Coord. Chem.* **2010**, *63* (13), 2349−2359.
(49) Fillaux, C.; Guillaumont, D.; Berthet, J.-C.; Copping, R.; Shuh, D. K.; Tyliszczak, T.; Auwer, C. D. Investigating the electronic structure and bonding in uranyl compounds by combining NEXAFS spectroscopy and quantum chemistry. *Phys. Chem. Chem. Phys.* **2010**, *12* (42), 14253.

https://dx.doi.org/10.1021/acs.inorgchem.0c00439
Inorg. Chem. XXXX, XXX, XXX−XXX